Cent. Eur. J. Geosci. • 6(4) • 2014 • 476-491
DOI: 10.2478/s13533-012-0192-x

VERSITA

Central European Journal of **Geosciences**

Fluid-rock interaction in the Kangankunde Carbonatite Complex, Malawi: SEM based evidence for late stage pervasive hydrothermal mineralisation

Topical issue

Raymond A. Duraiswami*, Tahira N. Shaikh

Department of Geology, University of Pune, Pune 411 007

Received 30 January 2014; accepted 21 June 2014

Abstract: The Kangankunde Carbonatite Complex from the Cretaceous Chilwa Alkaline Province in southern Malawi contains ankeritic and siderite carbonatite that are affected by late stage remobilisation by a carbothermal or hydrothermal fluid. The coarse pegmatitic siderite carbonatite that hosts exotic minerals like monazite, synchysite, bastnasite, strontianite and apatite in vugs and cavities constitutes some of the richest rare earth deposits in the world. Besides these minerals, our studies reveal the presence of collinsite and aragonite from the siderite carbonatite. Fine drusy monazites are seen as overgrowths on thin veinlets of siderite within the rare earth mineralised zones. We present unambiguous SEM-based surface textural evidence such as presence of dissolution-corrosion features like etching along cleavage, solution channels, solution pits, sinstered scaly surface, etc. along with rare earth mineralisation that suggests the exotic minerals in the siderite carbonatite did not crystallise from carbonate magma and are a result of sub-solidus processes involving carbonatite-derived fluids. We believe that the monazite-synchysite-bastnasite-strontianite-collinsite assemblages were formed by juvenile post magmatic hydrothermal alteration of pre-existing carbonatite by a complex CO_2-rich and alkali chloride-carbonate-bearing fluid at ~250 to 400°C in an open system. This late 'magmatic' to 'hydrothermal' activity was responsible for considerable changes in rock texture and mineralogy leading to mobility of rare earth elements during fluid-rock interaction. These aspects need to be properly understood and addressed before using trace and rare earth element (REE) geochemistry in interpreting carbonatite genesis.

Keywords: RE mineralisation • Scanning Electron Microscopy • monazite • synchysite-(Ce) • hydrothermal fluids • fluid-rock interaction • carbonatite • Kangankunde • Malawi

1. Introduction

Carbonatites are rare, peculiar igneous rocks formed by unusual processes [1]. Carbonatite melts are characterised by very low magmatic temperatures (~800 to 900°C) at atmospheric pressures and very low (0.008 to 0.03 PaS) viscosities [2, 3]. High concentrations of Sr, Ba, Th, U, P and light rare earth elements (LREE) are typical of carbonatite geochemistry [4]. Their classification is based primarily on modal mineralogy (calcite carbonatite; coarse grained-sövite; fine grained- alvikite, beforsite, etc.) or major oxide geochemistry (calcio-, magnesio-, ferro-carbonatite) [5]. Rare Earth (RE) carbonatite [6] are fine grained, pegmatitic or porphyritic varieties containing modal RE minerals as-

*E-mail: raymond.duraiswami@gmail.com

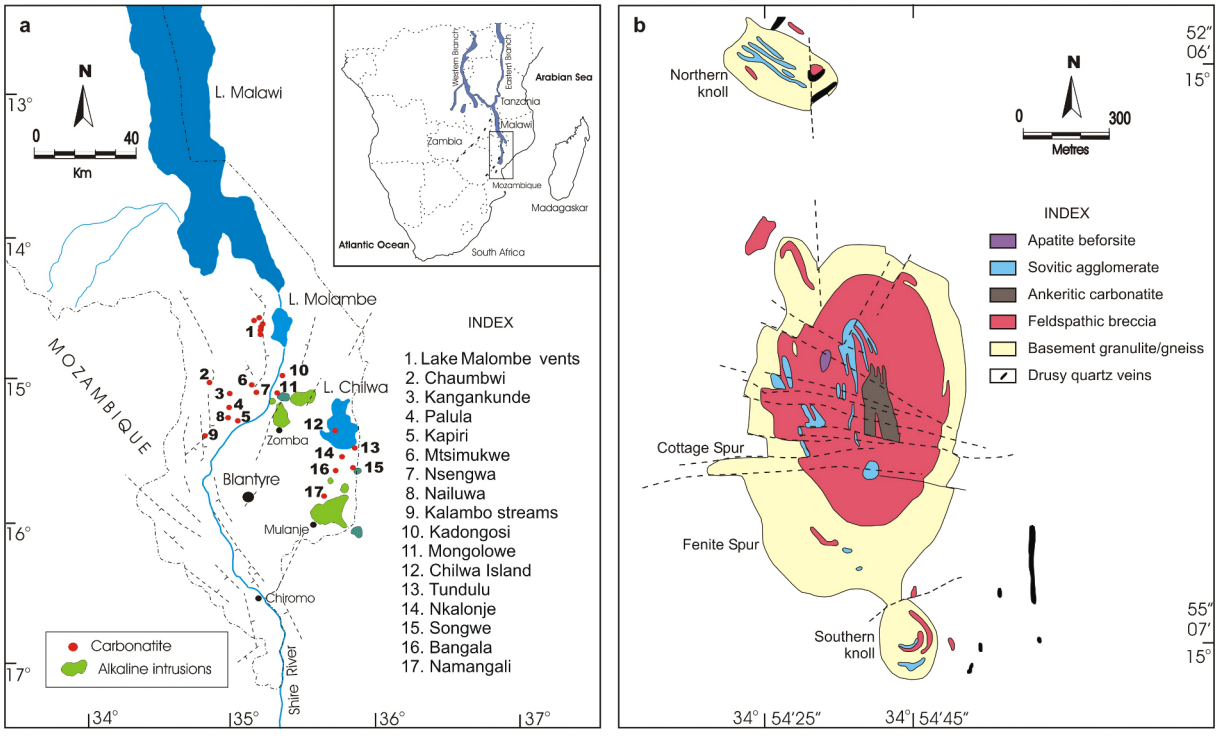

Figure 1. a) Map of southern Malawi showing the location of carbonatite intrusions. b) Geological map of Kangankunde Carbonatite Complex, Malawi [24].

sociated with variable Ca:Mg:Fe carbonatites with a whole rock value of >1% RE_2O_3. Carbonatite magmas are considered to be residual melts of fractionated carbonated nephelinite or melilitite [7, 8] or immiscible melt fractions of CO_2-saturated silicate melt [9–14]. Carbonatites are also considered primary mantle melts generated through partial melting of CO_2-bearing peridotite [15–19]. They are subdivided into primary magmatic carbonatites and carbothermal residual carbonatites formed from low temperature fluids that are rich in CO_2, H_2O and fluorine [20].

Although carbonatite magmas have formed from primary melts or as immiscible melt fractions of CO_2-saturated silicate melt, the associated RE carbonatite are considered to be a late 'magmatic' to 'hydrothermal' event [21–29]. Evidence for the hydrothermal origin for the RE mineralisation is based mainly on mineralogy, geochemistry and isotopes. Good descriptions of textural evidence using back-scattered electron images suggesting hydrothermal origin exist in literature for Barra do Itapirapuã (Brazil) [30] and Amba Dongar (India) [31], but such evidence does not exist for the Kangankunde Carbonatite Complex, Malawi despite the rich RE mineralisation.

The Cretaceous Chilwa Alkaline Province [32, 33] in southern Malawi contains numerous carbonatite centers (Figure 1a), some of the most famous being the Chilwa Island, Tundulu Carbonatite Complex [34, 35] and Kangankunde Carbonatite Complex [36]. The rocks from the Kangankunde Carbonatite Complex, Malawi (Figure 1b) are unique and hosts exotic minerals like monazite, synchysite, bastnasite, strontianite and apatite that constitute one of the richest RE deposits (11 Mmt of material with 8.4% $SrCO_3$ and 1.9% rare-earth oxides) in the world [37]. The abundance of RE hosting minerals in the Kangankunde Carbonatite Complex provides an opportunity to undertake mineralogical and textural studies to elucidate the late stage 'hydrothermal' hypothesis. In this paper, we present conventional petrographic and Scanning Electron Microscopy (SEM) based surface textural evidences for late stage hydrothermal activity from the Kangankunde Carbonatite Complex. These studies suggests that initially the host carbonatite was pervasively impregnated by corrosive gases and fluids that resulted in formation of cavities, vugs and veins and culminated in widespread RE mineralisation due to streaming of late stage hydrothermal fluids.

2. Geology

The Kangankunde Carbonatite Complex is one of several carbonatite complexes in southern Malawi (Figure 1a) as-

sociated with the Shire Valley section of East African Rift System. The Kangankunde Hill is an eroded remnant of a carbonatite depocentre belonging to the Lower Cretaceous Chilwa Alkaline Province. The Kangankunde Carbonatite Complex differs significantly from other carbonatite in the marked absence of nepheline syenite and other silicate rocks like lamprohyres and melanephelinite. The carbonatite complex (Figure 1b) consists of faulted segments of concentric zones of fenites, carbonated agglomeratic breccias and strontianite-rich ankeritic carbonatite. Small plugs and dyke-like intrusions of 'apatite beforsite' are present in the Kangankunde Hill [21, 36]. In the central part of the complex, the carbonatite dykes or veins (stockwork?) follow an arcuate pattern, with a plug-like carbonatitic intrusion near the crest of the hill. The veins constituting the stockwork can be classified into five varieties:

1. Fine to medium grained dark brown siderite carbonatite.
2. Coarse grained light to dark brown mottled ankeritic/sideritic carbonatite with patches of RE minerals.
3. Whitish pale grey to light buff ankerite carbonatite.
4. Purplish black to dark brown siderite and Mn-rich ankerite carbonatite.
5. Creamy white to greenish grey strontianite rich carbonatite.

Outcrops of Mn-rich ankerite carbonatite occur in the central zone of the complex. The Mn-rich ankerite carbonatite is chocolate brown to black in appearance, massive with porous, earthy patches. The agglomerate consists of subrounded to rounded fragments of variably feldspatised rocks set in a white, fine grained calcite matrix. Towards the flanks of the central zone of the Kangankunde Carbonatite Complex, dark manganiferous ankerite with streaky bands is exposed. The rock shows apatite rich schlieren [38] and contains variable amounts of strontianite and monazite.
The rare earth mineralisation at Kangankunde occurs either as impregnations of monazite, pink florencite or flaky bastnasite throughout the carbonatite rock or as concentrations with different forms [21]. A significant but relatively uncommon form of RE concentration are small rounded to oval stocks of up to 1m with drusy or coarse grained rock (Figure 2a) containing monazite, barite, strontianite and ankerite veins (Figure 2b). The commonest type of monazite concentration occurs along sideritic margins of intrusive carbonatite dykes. Significant enrichment of monazite, strontianite, barite and quartz are also seen in cavities, small veins and veinlets in the carbonatite host (Figure 2c). The veins generally tend to pinch and swell, often assuming bulbous forms and terminations (Figure 2d). The RE mineralised veins show an irregular corrosive boundary with the host carbonatite. Sometime the RE mineralised veins show angular to rhombohedral contact that mimics the crystal form of siderite within the carbonatite (Figure 2e). Several veins have curvilinear forms with corrosive contacts (Figure 2f) indicating a post magmatic intrusive nature of the veins during the hydrothermal activity. Veins of pure strontianite are also present in the siderite carbonatite. Besides the carbonatite association, monazite also occurs with drusy quartz in the Northern and Southern Knoll (Figure 1b) and provides strong field evidence for late stage hydrothermal origin [21]. The fenitised country rocks around Kangankunde contain flesh coloured orthoclase, sodium amphibole, aegirine augite and monazite suggesting widespread pervasive hydrothermal mineralisation in the basement rocks.

3. Sampling and Methodology

The first author collected sideritic carbonatite (KAN1), sovitic agglomerate (KAN2), manganiferous sovitic carbonatite (KAN3, KAN4), ankeritic carbonatite (KAN5), Mn-rich ankerite carbonatite (KAN6), and sovite (KAN7, KAN8, KAN9) during his 1999 field visit to Kangankunde. In this paper, we present the petrographic descriptions for sovitic agglomerate, manganiferous sovitic carbonatite and siderite carbonatite. Three different rare earth mineralised vugs (K1, K2 and K3) from the siderite carbonatite (KAN1) were selected on basis of variation in colour and mineralogy for detailed X-ray studies. Mineral aggregates from these vugs were carefully scraped by a steel scalpel and care was taken not to include the host carbonatite. The scraped material was hand ground into fine powder in an agate mortar. The powders were subjected to XRD (Cu Kα radiation) at the Department of Physics, University of Pune. The X-ray powder diffraction data was collected over a range of 20°–65° 2Θ. The scraped mineral aggregates and host siderite carbonatite were carefully mounted on stubs and subjected to imaging and geochemical analyses using a energy-dispersive JEOL JSM-6360A Scanning Electron Microscope fitted with a LA electron microprobe (operating conditions: 20 kV accelerating voltage and beam diameter approximately 5 µm).

4. Petrography

The agglomerate at Kangankunde Hill consists of a calcite matrix with angular to subangular fragments of pink fenite, turbid feldspar and iron oxide with accessory quartz, barite

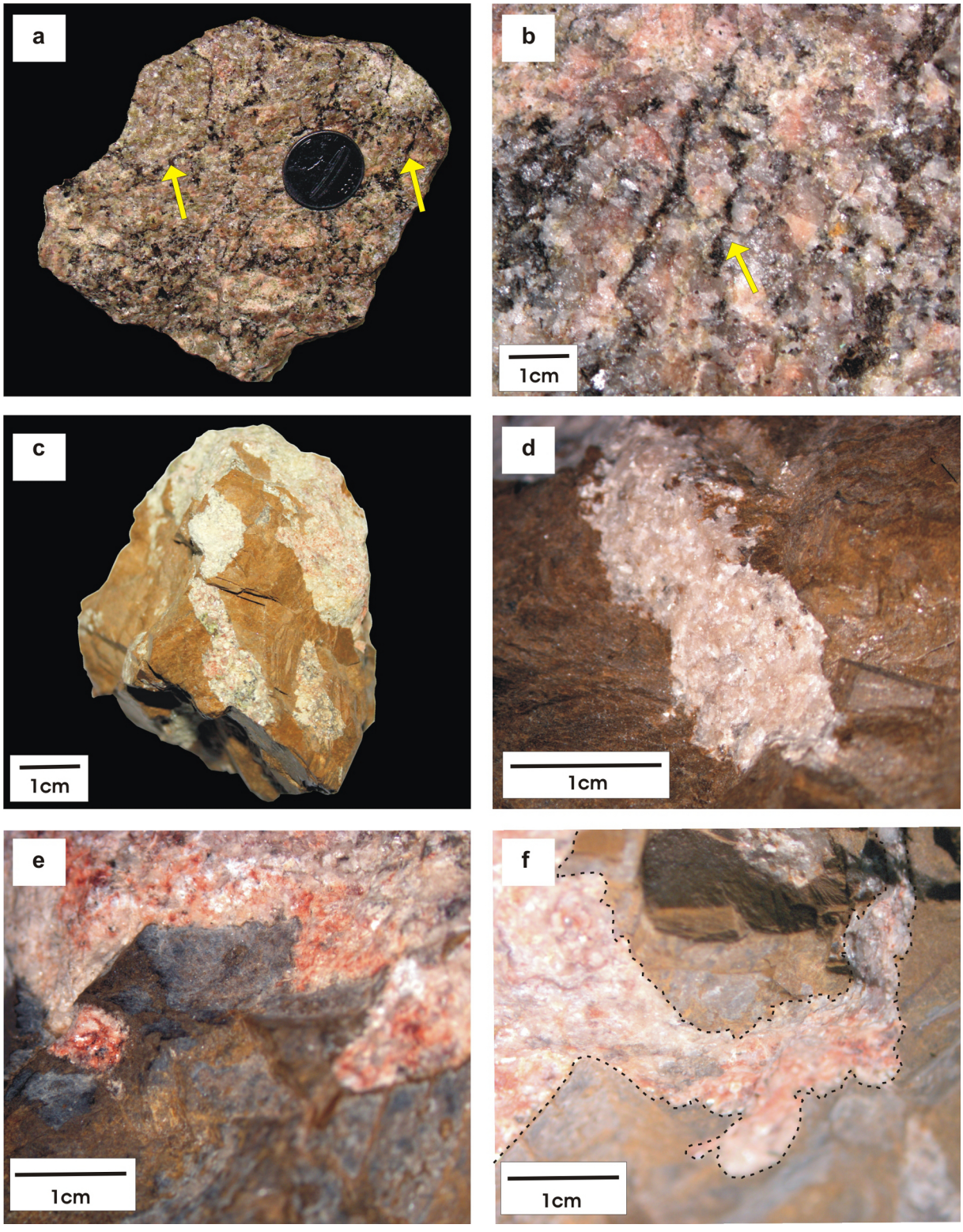

Figure 2. a) Hand specimen of RE carbonatite within small oval stocks in siderite carbonatite. Note the occurrence of fine ankerite veins marked by arrows. b) Close- up of RE carbonatite showing ankerite (brown), florencite (pink), monazite (green) and strontianite (white) mineralisation. c) Hand specimen of siderite carbonatite with veins of rare earth minerals. d) Close-up of bulbous termination of a RE mineralised vein. e) Angular to rhombohedral contact between the RE mineralised veins and siderite carbonatite. f) Curvilinear veins in the siderite carbonatite.

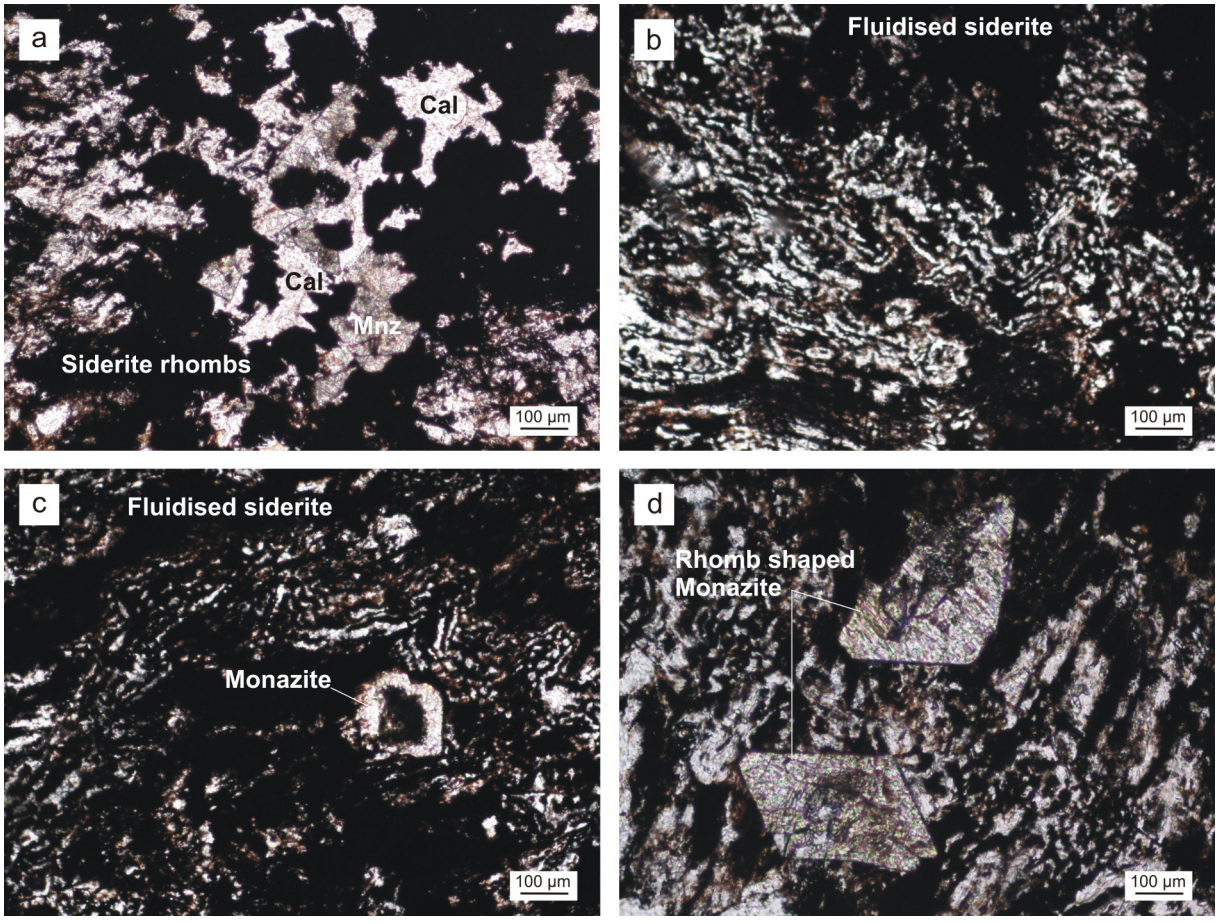

Figure 3. Photo micrographs: a) Siderite carbonatite showing euhedral to subhedral grains of siderite and coarse grained calcite and monazite. Note the change in texture towards the upper left and lower right corner of the photograph. b) Siderite carbonatite with fluidal structure. c) Euhedral monazite within the highly fluidal sideritic carbonatite. d) Rhomb shaped monazites in fluidised carbonatite.

and monazite. The siderite carbonatite occurs as two distinct varieties: A) fine-grained, dark brown, massive rock with a prevalent saccharoidal texture, and B) tawny, light brown, coarse to blocky variety with a predominantly pegmatitic texture.

The massive, fine grained, siderite carbonatite consist of abundant euhedral to subhedral rhombohedra of siderite and monazite that are set in a coarse grained clear calcite matrix (Figure 3a). In samples showing streaky texture, the siderites are anhedral and appear to be drawn into patterns that resemble fluidisation or streaming effect (Figure 3b). Occasionally, the streaming is disrupted by rhombohedral 'augen' of siderite. Wherever individual siderite 'augen' exists they have developed clear rims. Individual monazite crystals or group of crystals are also sometimes seen within the fluidised sideritic matrix (Figure 3c,d). Most features seen in the streaky siderite carbonatite indicate late stage interaction and remobilisation due to a carbothermal or hydrothermal fluid.

The coarse grained, pegmatitic sideritic carbonatite contain enclaves of RE minerals and quartz. Thin veinlets of siderite crystals are occasionally seen in the quartz enclaves. Many of the siderite veins show overgrowths of fine drusy monazite (Figure 4a). Flaky synchysite and bastnasite are seen in close proximity to the siderite veins. More commonly, the monazite crystals occur as colourless to pale brown aggregates in a quartz matrix (Figure 4b). Individual monazite crystals are 10 to 300 µm long, euhedral, prismatic and their colour varies from colourless, pistachio green to brown (Figure 4c). The colour variation is not related either to their chemistry or different varieties of host carbonatite [38]. Monazites cut perpendicular to c-axis are six-sides (Figure 4d). The cores of most monazite crystals are cloudy and perforated due to α-track emissions from uranium decay. A weak zoning is seen in some of the larger crystals, but these are unlike those reported by Cressey et al. [39] using SEM micrographs.

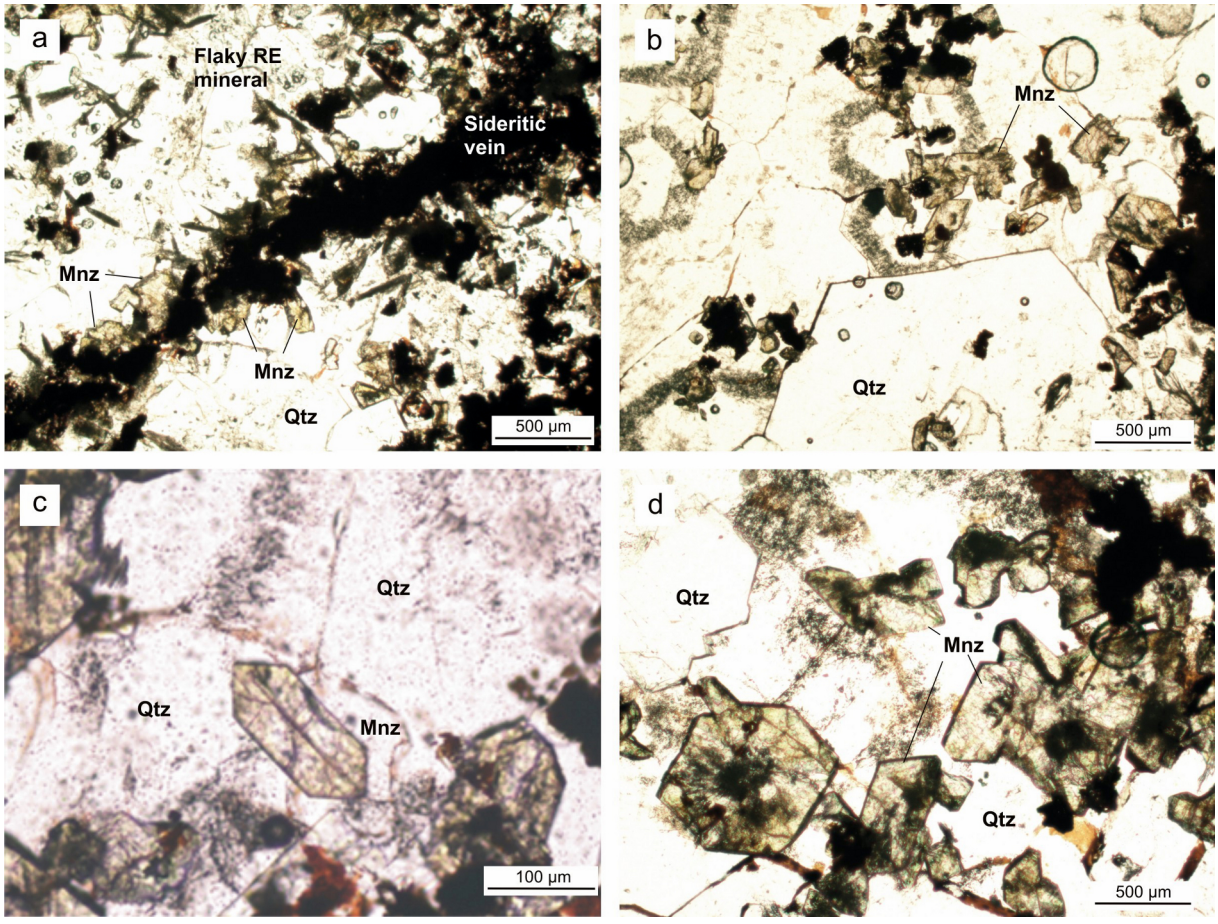

Figure 4. Photo micrographs of quartz vein within carbonatite. a) Siderite veins with overgrowths of drusy monazites. b) Aggregates of euhedral to subhedral monazite crystal within late stage euhedral to subhedral quartz. c) Euhedral prismatic crystal of green monazite. d) Six sided monazite within quartz rich matrix.

5. X-ray diffraction

RE minerals identified in X-ray powder diffraction patterns from three samples (K1, K2, and K3) is presented in Figure 5 and the identified phases are given in Table 1. Synchysite [Ca (Ce, La) $(CO_3)_2F$] is present in samples K1 and K3. The 100% peak of synchysite overlaps with that of strontianite [$SrCO_3$] in samples K1 and K3 whereas 64% of synchysite, 59% and 56% peaks of bastnasite [(Ce, La) $(CO_3)F$] also overlaps with that of strontianite in sample K3. Strontianite is identified in sample K1 and K3 while monazite [(Ce, La, Nd, Th) PO_4] is identified in sample K1 and K2. Bastnasite is identified in all three samples (K1, K2 and K3) making it the most common RE mineral. Aragonite [$CaCO_3$] is identified in two samples (K1, K2). Some minor peaks of parasite (2.84 d°A, 53%; 1.5418 d°A, 28%) and pyrochlore (3.1104 d°A, 50%; 1.8483 d°A, 18%) are also seen in sample K3. The RE flourcarbonates bastnasite, synchysite and parasite have similar crystal structures wherein (CeF) and (Ca) layers are separated by (CO_3) layers along the (001) plane [40]. Structural refinement reveal differences between bastnasite (hexagonal), synchysite (pseudo-hexagonal) and parasite (monoclinic) due to the presence of (Ca) layers in the lattice [41–43]. Intergrowth of syntactically oriented phases [44] is therefore quite common in these minerals as they have similar structures with identical growth-surfaces between (CeF) and (CO_3) layers. According to the isobaric-isothermal diagrams of William-Jones and Wood [45] the pairs bastnasite-synchysite, bastnasite-parasite and parasite-synchysite are quite common, whereas the three-phase assemblage is metastable. From the XRD analyses carried out by us, it is clear that the bastnasite-synchysite association is most common, possibly indicating syntactical intergrowth similar to those seen in the BSE images from Barra do Itapirapuã (Brazil) [30] and Amba Dongar (India) [31]. However, the possible presence of bastnasite-synchysite-parasite in sample K3 could suggest a three-phase metastable assemblage.

Table 1. X-Ray Diffraction data for identified phases from the mineral aggregates.

Sample No.	Mineral	(d°A)	I/Imax (%)
K1	Synchisite	3.5339	100
		4.5291	58
		1.8769	23
	Aragonite	3.4399	77
		1.9811	37
		2.7223	25
	Bastnasite	2.8847	61
		4.8742	69
		2.4487	50
		2.5923	26
	Monazite	3.0998	51
		2.8400	37
		3.3143	58
		4.1907	52
	Strontianite	3.0079	50
		2.0490	40
		1.9028	37
		1.8207	32
		2.5495	29
		1.9450	29
K2	Monazite	3.0998	100
		4.1907	75
		4.0953	71
		3.3143	85
		3.5201	63
		2.5996	33
		2.8666	48
		2.1414	36
	Aragonite	3.4399	91
		2.7303	45
		2.4813	33
		2.3266	26
		2.1080	59
		1.9729	23
		1.7430	30
	Bastnasite	3.5758	72
		2.0579	33
		1.6731	28
		1.4367	22
K3	Synchisite	3.5339	100
		3.3264	50
		2.0534	64
		2.0187	35
		1.945	32
		1.8207	43
	Strontianite	3.4399	98
		3.0079	45
		2.4813	54
	Bastnasite	2.8847	78
		2.5923	34
		2.8847	78
		2.4487	59
		2.0987	37
		1.8953	56
		1.5703	26
	Parisite	2.84	53
		1.5418	28

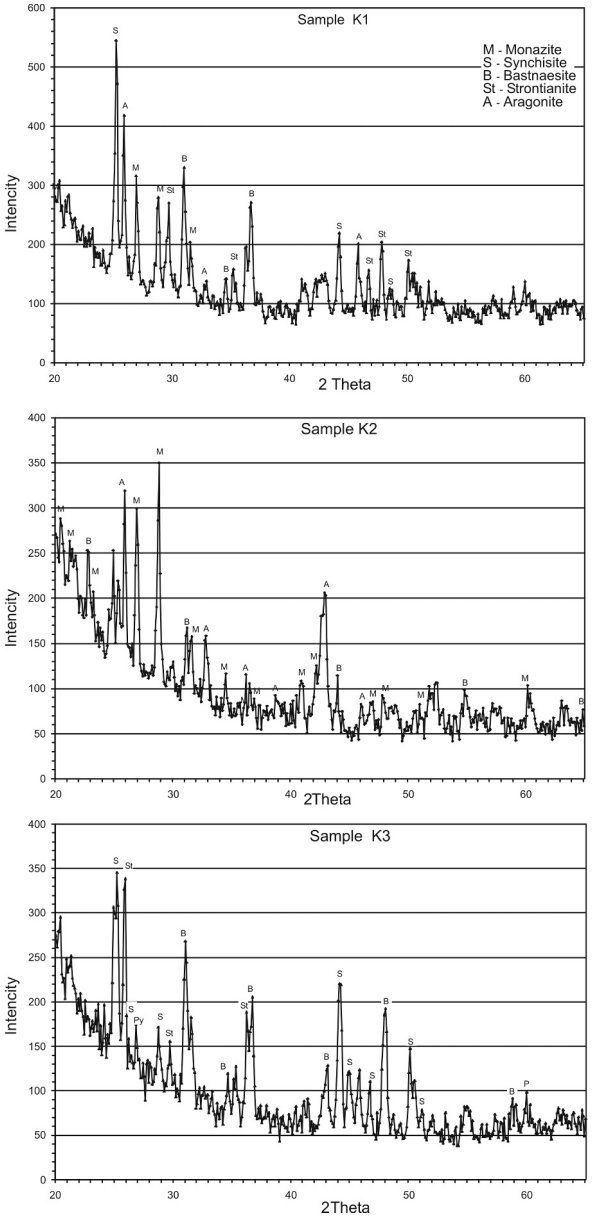

Figure 5. X-ray diffractogram of the mineral aggregate from Kangankunde Carbonatite Complex, Malawi.

6. SEM-EDX studies

The SEM micrographs of host siderite carbonatite show anhedral to subhedral crystals of siderite in fresh, unaltered specimens. Most siderite crystals occur as rhombohedra with curved crystal faces (Figure 6a). Some of the large crystals are characterised by sub conchoidal fracture pattern. Few large scalenohedron of siderite have grown into vugs and fracture planes. Hydrothermally altered siderite carbonatite occur along cleavage planes and frac-

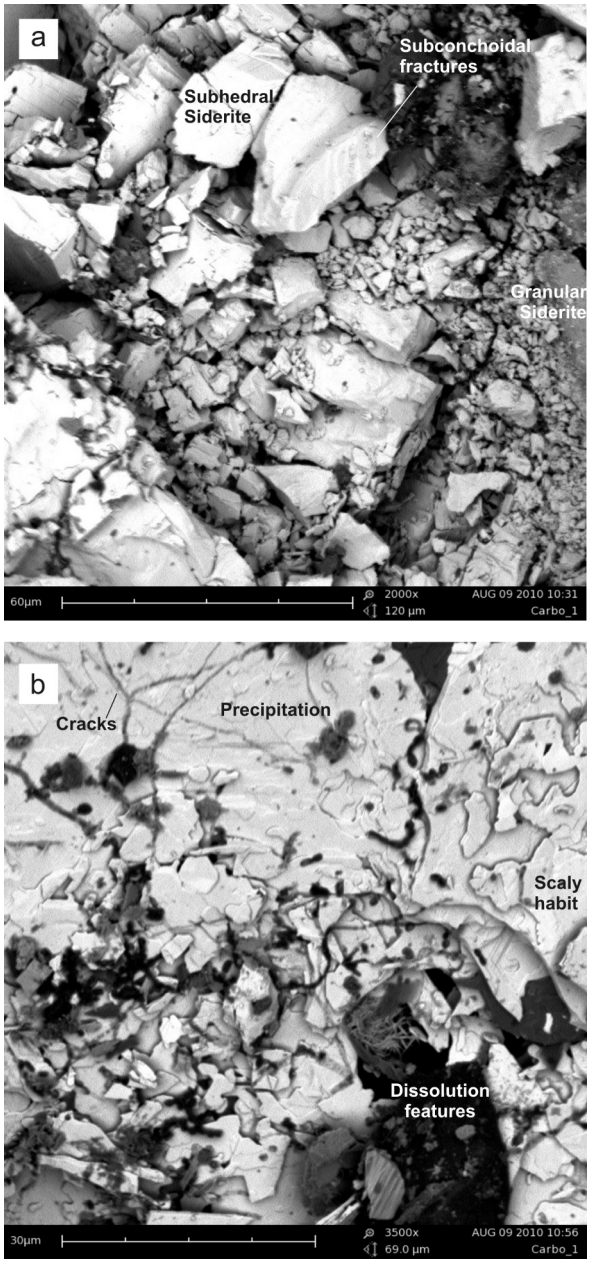

Figure 6. SEM micrographs showing: a) Subhedral to anhedral siderite crystals. Note the variable grain size and the conchoidal fracture pattern on the larger grain. b) Scaly precipitation flakes of carbonate formed due to corrosion and subsequent precipitation of carbonate under influence of hydrothermal fluids.

tures. Samples from these zones do not show the granular, anhedral to subhedral character of the unaltered siderite carbonatite. SEM of the remobilised siderite carbonatite shows either a smooth massive or scaly, sinstered surface with several cracks (Figure 6b). The smooth surfaces have developed where corrosion is complete followed by precipitation of siderite. Partial corrosion or dissolution of pre-crystallised siderite lends a granular appearance. Formation of granular and scaly crackled surface texture is interpreted by us as an effect of corrosion of pre-existing crystalline siderite carbonatite followed by precipitation under the influence of post emplacement magmatically related hydrothermal solution (carbothermal solution?).

Evidence for corrosion from solution also comes in the siderite carbonatite where solution channels are seen along possible cleavage planes and irregular cracks (Figure 7a). In the vicinity of such solution channels the surface of the siderite appears spongy and pitted due to minute solution pits. Precipitation occurs elsewhere on the flat surface of siderite (e.g. lower half of Figure 7a). Etching and dissolution of carbonate is also seen along two sets of cleavage (Figure 7b). Generally, maximum corrosion is seen along edges of crystals with smooth un-etched surface along the cleavage plane. Sometimes the smooth cleavage plane of siderite is disrupted by 'v' pits formed by chemical etching. The siderite carbonatite also contains large solution channels and irregular vug-like solution features (Figure 7c) connected to fractures. The walls of such features show small solution pits. High relief solution features in the form of small rhombohedra with upturned carbonate precipitation on edges is seen in the vicinity of the solution channels. The siderite carbonatite also shows large solution cavities with monazite crystals in the center (Figure 7d). The walls of such cavities contain solution pits of various diameters.

SEM micrographs of the siderite carbonatite also reveal the presence of the mineral collinsite [Ca_2 (Mg, Fe^{2+}) $(PO_4)_2.2H_2O$]. Collinsite is generally associated with small vugs and fissures in the altered siderite carbonatite. In hand specimens, the mineral is hardly visible as it has the same tawny or brown colouration as the host carbonatite. In SEM micrographs the mineral occurs as fibrous aggregates (Figure 8a). In places, serrate tufts of collinsite are also present. At higher magnifications, the collinsite aggregates show a bladed habit (Figure 8b); individual sheaves or fibers are elongated along (100). Collinsite has well developed cleavage along (010). The morphological characteristics of collinsite from the present study are similar to that reported from Rapid Creek and Big Fish River area Yukon Territory, and the Kovdar Carbonatite Complex, Northwestern Russia [46, 47].

The rare earth mineralisation in cavities and vugs from the siderite carbonatite were also investigated by SEM studies. Fine radiating aggregates of fibrous synchysite are seen to grow on the siderite carbonatite (Figure 9a). At higher magnifications, synchysite occurs as pseudo-hexagonal stacks with splintery fracture habit (Figure 9b). Occurrence of synchysite is common where maximum effects of corrosion and precipitation are seen. The host

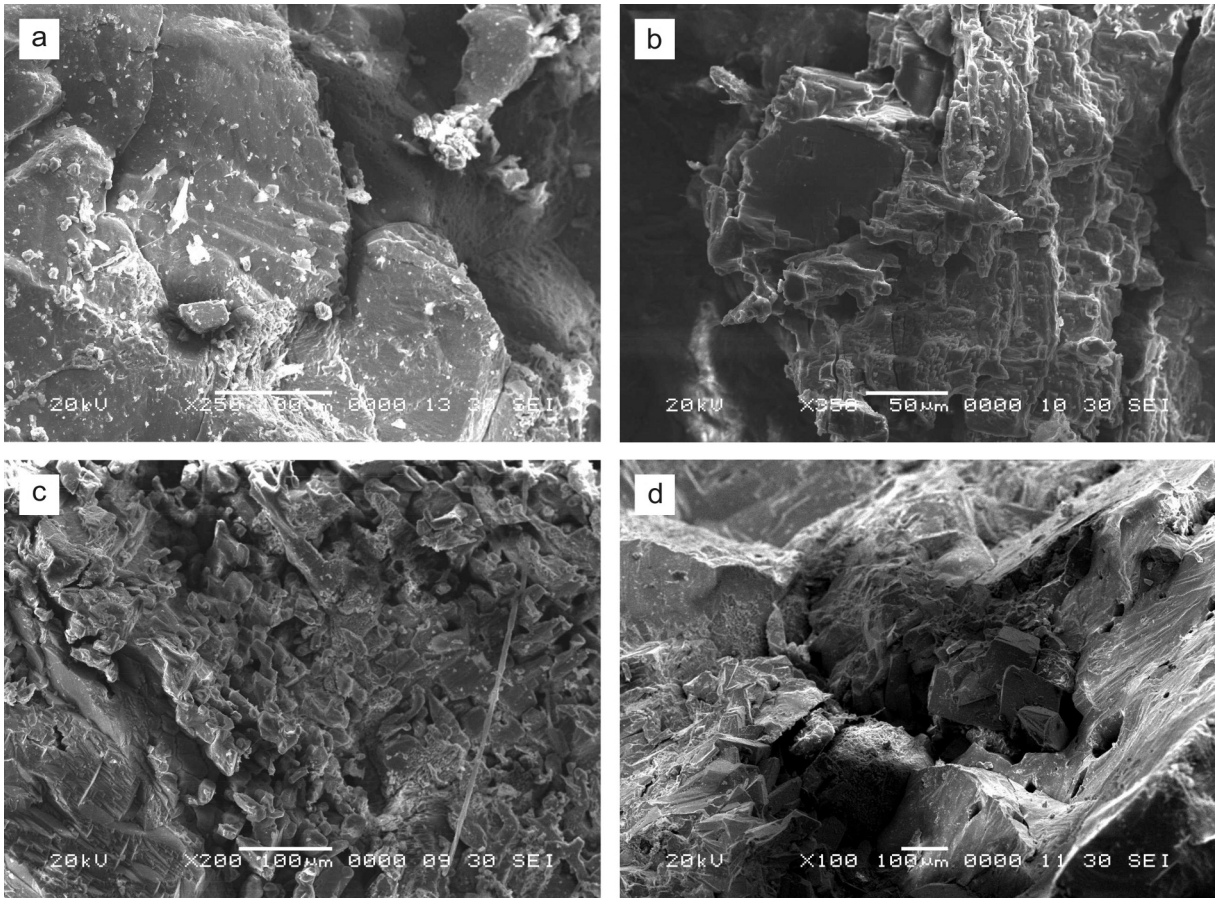

Figure 7. SEM micrographs of host siderite carbonate. a) Solution channels along possible cleavage planes and irregular cracks. Note the spongy pitted surface on the upper central part of the micrograph and precipitation on the flat mineral surface in the lower half. b) Etching and dissolution of carbonate along two sets of cleavage planes. Note the smooth surface of the cleavage plane in the mid-center of the upper left corner of the photomicrograph. c) High relief solution features producing the small rhombohedral patterns with upturned carbonate precipitation on edges. Note the large, irregular vug-like solution feature to the left of the micrograph showing small solution pits. d) Large solution cavity with monazite crystals in the center. The walls of the cavity show numerous solution pits.

carbonatite in such cases show subhedral scalenohedrons of siderite that have been corroded along crystal faces and edges by invading fluids.

The mineralised vugs in siderite carbonatite at Kangankunde contain drusy monazite veins (Figure 10a,b). Monazites occur as small prismatic crystals (Figure 10a) or as flattened crystals (Figure 10b) on (101). Crystal faces may be bound by (110) (see Figure 10c) and modified by the small development of (100) (Figure 10d). Individual crystals may show zoning (e.g. Figure 10d).

SEM studies also reveal the presence of a highly fibrous mineral (Figure 11a) that occurs as encrustations on siderite carbonatite. At higher magnifications, the mineral assumes a flaky character (Figure 11b) and shows solution pits and related precipitation akin to chemical dissolution and re-precipitation on etched quartz grains. SEM-EDX suggests it to be calcium-magnesium carbonate (C – 11.17 wt.%, O – 14.94 wt.%, Ca – 2.97 wt.%, Mg – 1.51 wt.%). Based on its morphology and chemistry we suspect this mineral to be aragonite. The presence of aragonite in the RE mineralised zones within the siderite carbonate has already been confirmed by us in the XRD studies. Occurrence of aragonite in carbonatites has been poorly reported in literature for obvious reasons as the mineral inverts to calcite with time.

The SEM-EDX chemical analyses of monazite, synchysite and siderite are presented in Table 2. The low totals reported in the analyses are within the data range for respective minerals in published literature [30, 48, 49]. The low totals are probably related CO_2, F and other volatiles in the RE- fluorocarbonates and monazites. Monazites from Kangankunde are typically low-Th with abnormally high concentrations of rare earth elements (REE). Monazites from the present study show low CaO (0.2–0.7 wt.%), and high MgO (0.86–2.52 wt.%), SiO_2 (2.28–6.39 wt.%), P_2O_5 (11.68–18.87 wt.%) and ZrOs (3.53–3.86 wt.%). The monazites

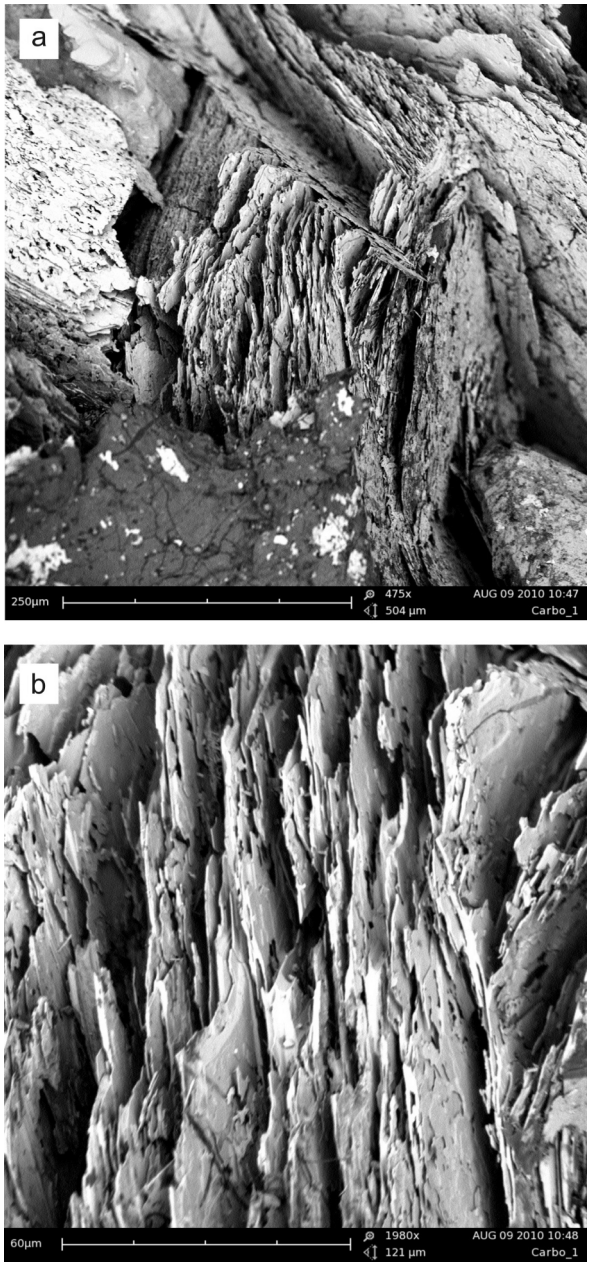

Figure 8. SEM micrographs. a) Collinsite aggregate in siderite carbonatite. b) Bladed, lath-like elongated collinsite crystals.

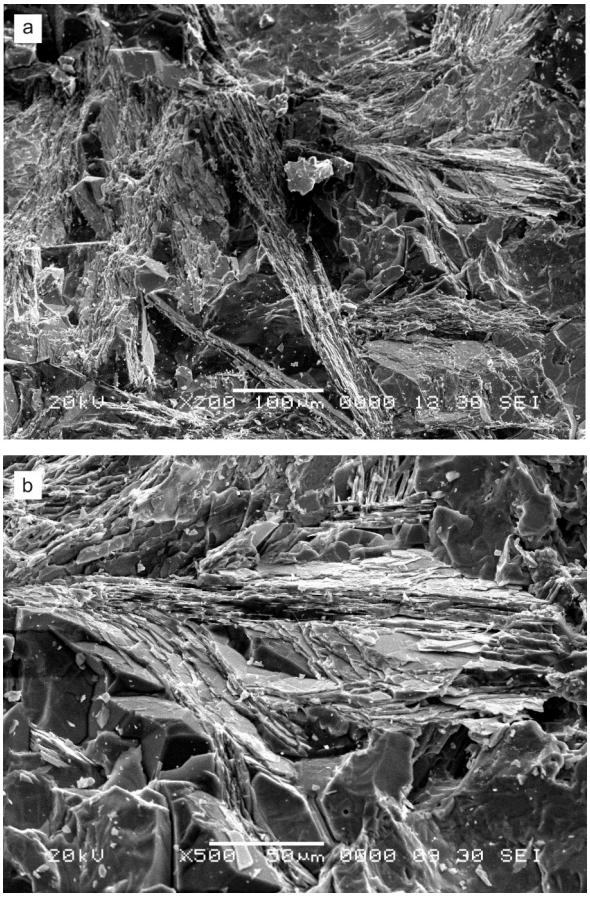

Figure 9. SEM micrographs. a) Fine radiating aggregates of fibrous synchysite are seen as encrustations on the siderite carbonatite. b) Pseudohexagonal stacks of splintery synchysite.

are also characterised by high La_2O_3 (0.61–9.58 wt.%), Ce_2O_3 (13.91–19.47 wt.%), Pr_2O_3 (1.71–2.52 wt.%), Nd_2O_3 (5.29–6.19 wt.%), Sm_2O_3 (1.03–14.86 wt.%), and Gd_2O_3 (13.34–21.44 wt.%). However, except for Sm_2O_3, there appears to be some uniformity in the distribution of rare earth elements in the studied monazites. Cressey et al. [39] reported sector-zoned monazites from Kangankunde with variation in La_2O_3 (up to 6.0 wt.%) and Nd_2O_3 (up to 3.9 wt.%) between sectors. According to them, sectors uptake REE preferentially e.g. La by (011) sector surfaces and is enhanced relative to that of ($\bar{1}$01) and (100) sectors and uptake of Nd is more easily facilitated on ($\bar{1}$01) and (100) surfaces relative to (011). Interestingly, Ce showed no partitioning differences and is uniformly distributed in the monazites. It is speculated that the typical chemistry of monazites from Kangankunde may be due to coupled substitutions involving REE, Ca, Th, Si or P in the monazite structure leading to solid solutions to a cheralite [(REE, Ca, Th) (P, Si)O_4] like phase [50].

The synchysite from the present study is characterised by variable amounts of CaO (0.12–0.25 wt.%), MgO (1.04–1.32 wt.%) and SiO_2 (2.53–4.8 wt.%). REE concentrations are variable (La_2O_3: 0.91–2.05 wt.%, Ce_2O_3: 2.08–3.48 wt.%, Pr_2O_3: 5.56–10.45 wt.%, Nd_2O_3: 0.39–0.74 wt.%, Sm_2O_3: 8.71–10.12 wt.%, Gd_2O_3: 11.95–15.09 wt.%, Dy_2O_3: 0.05–3.81 wt.%) and Yb_2O_3: 37.03–56.17 wt.%). In contrast, bastnasite shows higher La_2O_3 (22.7 wt.%), Ce_2O_3 (42.76 wt.%), Nd_2O_3 (11.67 wt.%) and lower Sm_2O_3 (2.33 wt.%), Gd_2O_3 (0.84 wt.%) and Yb_2O_3 (0.49 wt.%).

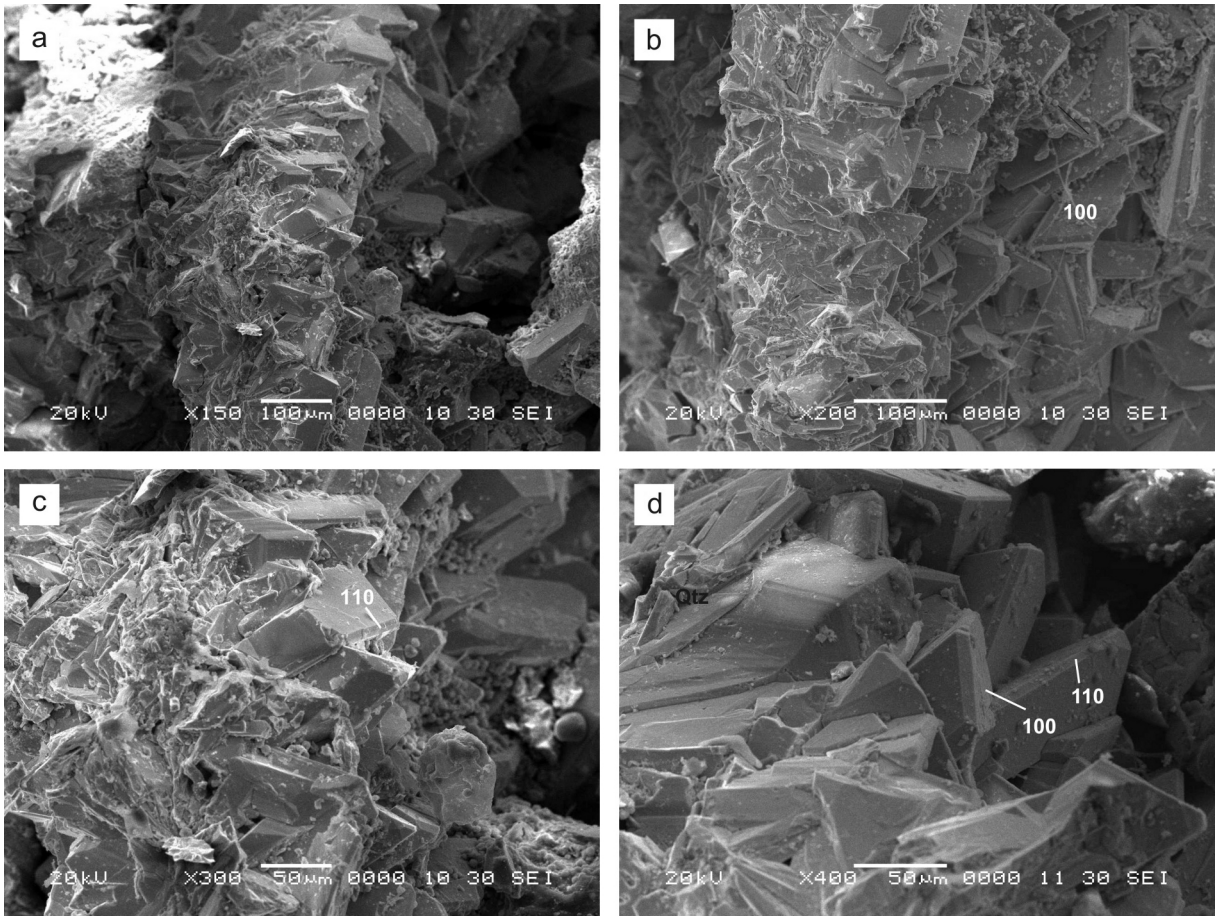

Figure 10. SEM micrographs of monazites showing drusy veins and crystal aggregates.

The $LREE_2O_3$ concentration range from 38.79 to 42.70 wt.% in monazites and 17.65 to 28.84 wt.% in synchisite. The highest $LREE_2O_3$ concentration of ~85 wt.% is seen in bastnasite (Table 2). The $HREE_2O_3$ concentration range from 13.34 to 24.71 wt.% in monazites and 55.93 to 68.17 wt.% in synchisite. Based on these analyses, it can be concluded that the concentration of $LREE_2O_3$ is relatively higher in the bastnasite and monazite when compared to synchisite where $HREE_2O_3$ seem to be preferentially concentrated. All the minerals analysed in the present study show the Ce>La>Nd order of preference for REE uptake. The heavy rare earth elements (HREE) tends to get preferentially concentrated in the synchisite and siderite (Yb_2O_3 – 3.81 wt.%; Lu_2O_3 – 10.36 wt.%).

7. Discussion

In this section we integrate our observations and findings with pre-existing evidence in published literature supporting the late stage 'hydrothermal' RE mineralisation. It is a well know fact that RE minerals are common in carbonatites, more so in rocks that formed late in the sequence of emplacement [51, 52]. Monazite bearing carbonatite are therefore considered to have formed at the later stages of emplacement. Exceptionaly high concentrations of REE in monazites, coupled with a very strong fractionation between the light and heavy REEs, suggests that the LREE either remained in the residual magma or they were concentrated within the last phase of carbothermal fluids [53]. The Kangankunde Carbonatite Complex consists of ankerite and siderite carbonatites characteristic of 'late stage' carbonatites. Abundant bright green monazite occurs throughout these carbonatites and is also associated with thick quartz veins [21, 34, 36] together with baryte, strontianite, bastnasite and florencite-goyazite that are believed to have been formed by a late stage activity at the magmatic-hydrothermal boundary [23]. The Sm/Nd isotopic evidence for Kangankunde [54] rocks links monazite and secondary apatite from carbonatites and fenites

Table 2. SEM-EDX analyses of monazite, synchisite, bastnasite and siderite from mineralized vugs, Kangankunde Carbonatite, Malawi.

Oxide (wt.%)	Monazite			Synchysite		Bastnasite	Siderite
	Mon1	Mon2	Mon3	Syn1	Syn2	Bas1	Sid1
SiO_2	3.07	6.39	2.28	4.80	2.53	0.17	0.12
La_2O_3	7.29	9.58	6.61	0.91	2.05	22.72	b.d.l
Ce_2O_3	15.86	19.47	13.91	2.08	3.48	42.76	0.11
Pr_2O_3	1.71	2.52	2.03	5.56	10.45	6.02	1.48
Nd_2O_3	5.57	6.19	5.29	0.39	0.74	11.67	b.d.l
Sm_2O_3	11.96	1.03	14.86	8.71	12.12	2.33	b.d.l
Gd_2O_3	21.44	13.34	21.40	11.95	15.09	0.84	b.d.l
Dy_2O_3	2.99	b.d.l	b.d.l	0.05	3.81	b.d.l	b.d.l
Yb_2O_3	b.d.l	b.d.l	b.d.l	56.17	37.03	0.49	3.81
Lu_2O_3	0.28	b.d.l	b.d.l	b.d.l	b.d.l	0.20	10.36
FeO	b.d.l	0.23	2.51	1.35	3.94	b.d.l	52.61
MgO	0.86	2.52	1.77	1.04	1.32	0.14	1.05
CaO	0.22	0.20	0.70	0.12	0.25	2.41	1.76
ZrO_2	3.53	3.86	3.85	b.d.l	b.d.l	2.81	b.d.l
ThO_2	b.d.l	b.d.l	b.d.l	b.d.l	0.02	0.01	b.d.l
UO_2	0.05	b.d.l	0.04	b.d.l	b.d.l	b.d.l	b.d.l
P_2O_5	14.57	18.87	11.68	0.38	b.d.l	b.d.l	b.d.l
Total	89.41	84.18	86.94	93.52	92.83	92.57	64.39
$LREE_2O_3$ (La-Sm)	42.39	38.79	42.70	17.65	28.84	85.50	1.59
$HREE_2O_3$ (Gd-Lu)	24.71	13.34	21.40	68.17	55.93	1.53	14.17
Si	0.6040	1.1311	0.4469	0.8166	0.4232	0.0283	0.0137
La	0.5290	0.6255	0.4779	0.0571	0.1265	1.3958	–
Ce	1.1425	1.2619	0.9983	0.1296	0.2131	2.6077	0.0046
Pr	0.1226	0.1625	0.1450	0.3446	0.6369	0.3653	0.0618
Nd	0.3915	0.3914	0.3704	0.0237	0.0442	0.6943	–
Sm	0.8111	0.0628	1.0041	0.5108	0.6988	0.1338	–
Gd	1.3870	0.7830	1.3909	0.6741	0.8370	0.0464	.–
Dy	0.1895	–	–	0.0027	0.2053	–	–
Yb	–	–	–	2.9145	1.8891	0.0249	0.1331
Lu	0.0166	–	–	–	–	0.0101	0.3585
Fe	–	0.0340	0.4114	0.1921	0.5511	–	5.0401
Mg	0.2522	0.6650	0.5172	0.2638	0.3291	0.0348	0.3023
Ca	0.0464	0.0379	0.1470	0.0219	0.0448	0.4301	0.0859
Zr	0.3386	0.3332	0.3680	–	–	0.2282	–
Th	–	–	–	–	0.0008	0.0004	–
U	0.0016	–	0.0013	–	–	–	–
P	2.1556	2.5118	1.7216	0.0486	–	–	–

Stoichiometry of monazite based on 16 oxygens, synchysite based on 7 oxygen atoms and siderite based on 6 oxygen atoms. Abbreviation: b.d.l.- below detection level.

with monazite, florencite and REE-rich apatite from quartz veins thereby suggesting strong involvement of late stage metasomatic fluids. According to Wall et al. [55], textural evidence such as the presence of pseudomorphs containing the RE mineral assemblage, veinlets and drusy cavities, indicate that fluid based RE mineralisation replaced earlier formed carbonates. Similar textural evidence for hydrothermal fluorocarbonate mineralisation is also seen in the carbonatites of Barra do Itapirapuã (Brazil) [30] and Amba Dongar (India) [31].

Field based evidence such as streaky flow and remobilisation features in the Mn-rich ankerite carbonatite and RE mineralised veins with irregular corrosive boundaries within the siderite carbonatite in the Kangankunde Carbonatite, Malawi suggests fluid-rock interaction and remobilisation due to late stage hydrothermal activity. Unambiguous petrographic and SEM based surface textures such as widespread etching along carbonate cleavage, solution channels, solution pits, sinstered scaly precipitations and RE mineralisation in the near vicinity are important evidences that support the field based observations. Thus the textural evidence provided in this study suggests that the RE minerals in the siderite carbonatite have not directly crystallized from magma and are a result of sub-solidus processes involving carbonatite-derived fluids. Result of sub-solidus experiments involving carbonatite-derived flu-

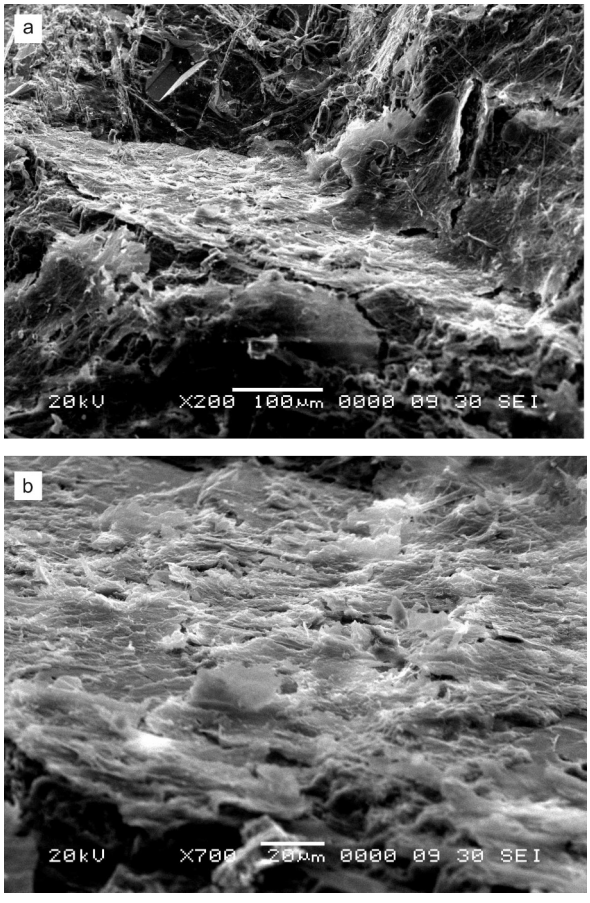

Figure 11. SEM micrographs of highly fibrous aragonite that occurs as encrustations on siderite carbonatite.

ids suggests that some RE minerals may directly precipitate, or may alter earlier minerals such as apatite [56]. Field and textural evidence from this study suggests that "hydrothermal" or "carbothermal" fluids or combinations of the two is pervasive into earlier formed carbonatites creating dissolution, corrosion and precipitation textures that ultimately produce RE mineral disseminations and schlieren in host carbonatite (e.g. sovite, ankerite carbonatite) or polycrystalline RE mineral aggregates in cavities, vugs and veins in siderite carbonatite. The hydrothermal fluids have also invaded the country rock or earlier formed fenites and transported away the REE [54, 56].

Evidence for later stage hydrothermal fluids also comes from fluid inclusions in quartz and fenites associated with the Kangankunde Carbonatite Complex. Carbonatitic fluids trapped as inclusions within recrystallised quartz contain traces of rare metal mineralisation (e.g. rutile, zircon, apatite, barites and cerussite?) as solid inclusions [57]. The fluids in the inclusions are complex CO_2-rich and alkali chloride-carbonate-bearing brines in which nahcolite ($NaHCO_3$), halite, calcite and burbankite are common daughter minerals. Such assemblages are considered to represent late-stage carbonatitic fluids reported from mineralised carbonatite complexes [58, 59].

The presence of collinsite in sideritic carbonatite from Kangankunde helped constrain the temperature of the hydrothermal fluids partaking in its genesis. In the Kovdor alkaline-ultramafic complex, northwestern Russia several generations of collinsite were formed by juvenile hydrothermal solutions derived from phoscorite and dolomite carbonatite [47]. Based on the relatively low f(CO_2) the upper limit of the hydrothermal process is set below 270–250°C, and is in agreement with the thermal range concerning the temperature of homogenisation of H_2O–CO_2 fluid inclusions in carbonatites [59]. The decrepitation temperature of liquid inclusions within post magmatically generated apatite is set at 270°C [60]. The temperate range also corresponds to the release of gaseous CO_2 from a carbonatite-derived fluid (carbotherm) that initially had dissolved 30–60 mol.% CO_2 [29, 61, 62].

Variability in the clumped isotope signature of carbonatites has been attributed to differences in mineralogy, water content, cooling rate and burial history. Based on inorganic precipitation experiments, Dennis and Schrag [63] believe that deviations from the original Ghosh et al. [64] calibration were due to precipitation of aragonite and amorphous carbonate instead of single-phase calcite. The presence of aragonite in the RE mineralised vugs from the present study could be possible proof that validates this hypothesis.

8. Conclusions

The siderite carbonatites from the Kangankunde Carbonatite Complex, Malawi occur as arcuate dykes within the sovitic agglomerate breccia. Streaky Mn-rich ankerite carbonatite show textural evidence of late stage remobilisation by carbothermal or hydrothermal fluids. Tawny, light brown, coarse pegmatitic siderite carbonatite hosts exotic RE minerals as disseminations or as aggregates in cavities and vugs. XRD studies of the mineral aggregates confirm the presence of monazite, synchysite, bastnasite, aragonite and strontianite. SEM micrographs of host siderite carbonatite show unambiguous textural evidence of fluid-host rock interaction in the form of dissolution-corrosion features, etching along cleavage, solution channels, solution pits, sinstered scaly surface, etc. along with precipitation of aragonite and rare earth minerals like monazite and synchysite. This indicates that at least some of the RE minerals did not crystallise from carbonate magma and are a result of sub-solidus processes involving carbonatite-derived fluids. The RE mineral assemblage were formed by

juvenile post magmatic hydrothermal alteration of carbonatite by a complex CO_2-rich and alkali chloride-carbonate-bearing fluid at ~250 to 400°C in an open system. Similar inferences have been drawn based on fluid inclusion, geochemical and isotope studies. The presence of collinsite from the siderite carbonatite from Kangankunde is probably recorded for the first time and further strengthens the hydrothermal alteration hypothesis. This late 'magmatic' to 'hydrothermal' activity was responsible for considerable changes in rock texture and mineralogy leading to mobility of REE during fluid-rock interaction. These aspects need to be properly understood and addressed before using trace and REE geochemistry in interpreting carbonatite genesis.

Acknowledgments

RAD thanks Prof. N.R. Karmalkar and Prof. N.J. Pawar for facilitating the visit to Malawi. We thank Mr. S.S. Shinde for his help with the SEM-EDX at the Department of Physics, University of Pune. Makrand Kale and Pradeep Kumar Sarkar are acknowledged for help in interpretation and discussions on the SEM micrographs. We also thank Prof. L.G. Gwalani, Michal Bucha, Dr. Ken Rogers and Dr. K.R. Randive for their support and encouragement and the two anonymous referees for their constructive reviews and helpful suggestions.

References

[1] Streckeisen A., Classification and nomenclature of volcanic rocks, lamprophyres, carbonatites and melilitic rocks. IUGS Subcomission on the Systematics of Igneous Rocks. Geol Rundsch, 1980, 69, 194–207

[2] Dobson D.P., Jones A.P., Rabe R., Sekine T., Kurita K., Taniguchi T., Kondo T., Kato T., Shimomura O., Urakawa S., In-situ measurement of viscosity and density of carbonate melts at high pressure. Earth. Planet. Sci. Lett., 1996, 143(1–4), 207–215

[3] Wolff J.A., Physical properties of carbonatite magmas inferred from molten salt data, and application to extraction patterns from carbonatite–silicate magma chambers. Geol. Mag., 1994, 131:145–153

[4] Nelson D.R., Chivas A.R., Chappell B.W., McCulloch M.T., Geochemical and isotopic systematics in carbonatites and implications for the evolution of ocean-island sources. Geochim. Cosmochim. Acta., 1988, 52, 1–17

[5] Woolley A.R., and Kempe D.R.C., Carbonatites: Nomenclature, average chemical compositions and element distribution. In: Bell K. (Ed.), Carbonatites: Genesis and Evolution. Unwin Hyman, London, 1989, 1–14

[6] Jones A.P., Genge M., Carmody L., Carbonate Melts and Carbonatites. Rev. Mineral. Geochem., 2013, 75, 289–322

[7] Gittins J., The origin and evolution of carbonatite magmas. In: Bell K. (Ed.), Carbonatites: Genesis and Evolution, Unwin Hyman, London, 1989, 580–600

[8] Gittins J., and Jago B.C., Differentiation of natrocarbonatite magma at Oldoinyo Lengai volcano, Tanzania. Mineral. Mag., 1998, 62, 759–768

[9] Freestone I.C., and Hamilton D.L., The role of liquid immiscibility in the genesis of carbonatites - An experimental study. Contrib. Mineral. Petrol., 1980, 73(2), 105–117

[10] Church A.A., and Jones A.P., Silicate-Carbonate Immiscibility at Oldoinyo-Lengai. J. Petrol., 1995, 36(4), 869–889

[11] Lee W.J., and Wyllie P.J., Liquid immiscibility between nephelinite and carbonatite from 1.0 to 2.5 GPa compared with mantle melt compositions. Contrib. Mineral. Petrol., 1997, 127(1), 1–16

[12] Dawson J.B., Peralkaline nephelinite-natrocarbonatite relationships at Oldoinyo Lengai, Tanzania. J. Petrol., 1998, 39(11–12), 2077–2094

[13] Halama R., Vennemann T., Siebel W., Markl G., The Gronnedal-Ika carbonatite-syenite complex, South Greenland: carbonatite formation by liquid immiscibility. J. Petrol., 2005, 46(1), 191–217

[14] Brooker R.A., and Kjarsgaard B.A., Silicate-carbonate liquid immiscibility and phase relations in the system SiO_2-Na_2O-Al_2O_3-CaO-CO_2 at 0.1–2.5 GPa with applications to carbonatite genesis. J. Petrol., 2011, 52(7–8), 1281–1305

[15] Wallace M.E., and Green D.H., An experimental determination of primary carbonatite magma composition. Nature, 1988, 335, 343–346

[16] Sweeney R.J., Carbonatite melt compositions in the Earth's mantle. Earth. Planet. Sci. Lett., 1994, 128(3–4), 259–270

[17] Harmer R.E., and Gittins J., The Case for Primary, Mantle-derived Carbonatite Magma. J. Petrol., 1998, 39(112), 1895–1903

[18] Harmer R.E., Lee C.A., Eglington B.M., A deep mantle source for carbonatite magmatism; evidence from the nephelinites and carbonatites of the Buhera district, SE Zimbabwe. Earth. Planet. Sci. Lett., 1998, 158, 131–142

[19] Yang K-F, Fan H-R, Santosh F., Hu F.F., Wang K-Y., Mesoproterozoic carbonatitic magmatism in the Bayan Obo deposit, Inner Mongolia, North China: constraints for the mechanism of super accumulation

of rare earth elements. Ore Geol. Rev., 2011, 40(1), 122–131

[20] Mitchell R.H., Carbonatites and carbonatites and carbonatites. Can. Mineral., 2005, 43(6), 2049–2068

[21] Garson M.S., Campbell-Smith W., Carbonatite and agglomeratic vents in the Western Shire Valley. Geol. Surv. Malawi, 1965, Memoir 3

[22] Gieré, R., Formation of rare earth minerals in hydrothermal systems. In: Jones A.P., Wall F., and Williams C.T. (Eds.), Rare Earth Minerals: Chemistry, Origin and Ore Deposits Chapman & Hall, London, 1996, 105–150

[23] Wall F., and Mariano N., Rare earth minerals in carbonatites: a discussion centered on the Kangankunde carbonatite, Malawi. In: Jones A.P., Wall F., and Williams C.T. (Eds.), Rare Earth Minerals: Chemistry, Origin and Ore Deposits Chapman & Hall, London, 1996, 193–225

[24] Smith M.P., Henderson P., Campbell L.S., Fractionation of the REE during hydrothermal processes: constraints from the Bayan Obo Fe–REE–Nb deposit, Inner Mongolia, China. Geochim. Cosmochim. Acta., 2000, 64, 3141–3160

[25] Yang Xueming, and Le Bas M.J., Chemical compositions of carbonate minerals from Bayan Obo, Inner Mongolia, China: implications for petrogenesis. Lithos, 2004, 72, 97–116

[26] Ngwenya B.T., Hydrothermal rare earth mineralisation in carbonatites of the Tundulu complex, Malawi: processes at the fluid/rock interface. Geochim. Cosmochim. Acta., 1994, 58, 2061–2072

[27] Andrade F.R.D., Möller P., Lüders V., Dulski P. and Gilg H.A., Hydrothermal rare earth elements mineralisation in the Barra do Itapirauã carbonatite, southern Brazil: behavior of selected trace elements and stable isotopes (C, O). Chem. Geol., 1999, 155, 91–113

[28] Ruberti E., Castorina F., Censi P., Comin-Chiaramonti P., Gomes C.B., Antonini P., Andrade F.R.D., The geochemistry of the Barra do Itapirapuã carbonatite (Ponta Grossa Arch, Brazil): a multiple stockwork. Am. Earth Sci., 2002, 15, 215–228

[29] Zaitsev A., Sinai Yu. M., Chakhmouradian A.R., Lepekhina E.N., Pyrrhotite–pyrite association in carbonatite series rocks of Khibina alkaline massif. Zap. Vser. Mineral. Obshchest, 1998, 127(4), 110–119 (in Russian)

[30] Ruberti E., Enrich G.E., Comin-Chiaramonti P.C.B., Gomes C.B., Hydrothermal rare earth mineralisation in the Barra do Itapirapuã (Brazil), multiple stockwork carbonatite. Can. Mineral., 2008, 46, 901–914

[31] Doroshkevich A.G., Viladkar S.G., Ripp G.S., Burtseva M.V., Hydrothermal REE mineralisation in the Amba Dongar carbonatite complex, Gujarat, India. Can. Mineral., 2009, 47, 1105–1116

[32] Woolley A.R., Lithosphere metasomatism and the petrogenesis of the Chilwa Province of alkaline igneous rocks and carbonatites, Malawi. J Afr. Earth Sci., 1987, 6, 891–898

[33] Woolley A.R., The Chilwa alkaline igneous province of Malawi: a review. In: Kampunzu A.B., Lubala R.T. (Ed.), Magmatism in Extensional Structural Settings. The Phanerozoic African Plate, Springer Verlag, Berlin, 1991, 377–409

[34] Garson M.S., Carbonatites in Malawi. In: Tuttle, O.F. and Gittins, J. (Eds.), Carbonatites. Interscience Publishers (John Wiley & Sons), New York, 1966, 33–71

[35] Karmalkar N.R., Duraiswami R.A., Hoffman A., Unusual rift related carbonatite magmatism from Southern Malawi, Southeast Africa and its implications in crustal evolution. In: Karmalkar N.R., Duraiswami R.A., Pawar N.J., Sivaji Ch. (Eds.), Origin and evolution of the Deep Continental Crust, Narosa Publishing House, New Delhi, 2010, 153–172

[36] Holt D.N., The Kangankunde Hill rare earth prospect-results of an economic investigation. Geological Survey Department, Ministry of Natural Resources, Government of Malawi. Bull. No. 20, 1965, 1–130

[37] King A.L., The mineral industry of Malawi. Minerals yearbook: mineral industries of Africa, Bureau of Mines, 1991, 3, 158–163

[38] Wall F., and Mariano A.N., Rare earth minerals in carbonatites: a discussion centered on the Kangankunde carbonatite, Malawi. In: Jones A.P., Wall F., Williams C.T., (Eds.) Rare Earth Minerals: Chemistry, Origin and Ore Deposits. Chapman & Hall, London, U.K. 1996, 193–225

[39] Cressey G.C., Wall F., Cressey A.A., Differential REE uptake by sector growth of monazite. Mineral. Mag., 1999, 63(6), 813–828

[40] Donnay G., and Donnay J.D.H., The crystallography of bastnäsite, parisite, röntgenite and synchysite. Am. Mineral., 1953, 38, 932–963

[41] Ni Yunxiang, Hughes J.M., Mariano A.N., The atomic arrangement of bastnäsite-(Ce), $Ce(CO_3)F$, and structural elements of synchysite-(Ce), röntgenite-(Ce), and parisite-(Ce). Am. Mineral., 1993, 78, 415–418

[42] Ni Yunxiang, Post J.E., Hughes J.M., The crystal structure of parisite-(Ce), Ce_2CaF_2 $(CO_3)_3$. Am. Mineral., 2000, 85, 251–258

[43] Wang Liben, Ni Yunxiang, Hughes J.M., Bayliss P., Drexler J.W., The atomic arrangement of synchysite-(Ce), $CeCaF(CO_3)_2$. Can. Mineral., 1994, 32, 865–871

[44] Bone V.I., On the terminology of the phenomena of mutual crystal orientation. Acta Crystallogr., 1972, A28, 508–512

[45] Willams-Jones A.E., and Wood S.A., A preliminary petrogenetic grid for REE fluorocarbonates and associated minerals. Geochim. Cosmochim. Acta., 1992, 56, 725–738
[46] Robinson G.W., Van Velthuisen J., Ansell H.G., Sturman B.D., Mineralogy of the Rapid Creek and Big Fish River area, Yukon Territory. Mineral. Rec., 1992, 23, 1–47
[47] Liferovich R.P., Pakhomovsky Y.A., Bogdanova A.N., Balaganskaya E.G., Pakhomovsky Y.A., Bogdanova A.N., Balaganskaya E.G., Chukanov N.V., Collinsite in hydrothermal assemblages related to carbonatites in the Kovdor Complex, Northwestern Russia. The Can. Mineral., 2001, 39, 1081–1094
[48] Zambezi P., Hale M., Voncken J.H.L., Touret J.L.R., Bastnäsite-(Ce) at the Nkombwa Hill carbonatite complex, Isoka District, northeast Zambia. Mineral. Petrol., 1997, 59, 239–250
[49] Förster H.J., Synchysite-(Y)–synchysite-(Ce) solid solutions from Markersbach, Erzgebirge, Germany: REE and Th mobility during high-T alteration of highly fractionated aluminous A-type granites. Mineral. Petrol., 2001, 72, 259–280
[50] Burt D.M., Compositional and phase relations among rare earth elements. In: Lipin B.R., and McKay, G.A. (Eds.), Geochemistry and mineralogy of rare earth elements. Rev. Mineral., 1989, 21, 259–307
[51] Kapustin Yu. L., Mineralogy of carbonatites. Amerind Publishing, New Delhi, 1980, 259 (Translated from Russian: Mineralogiya Karbonatitov, 1971) Nauka Publishers, Moscow
[52] Le Bas M.J., Diversification of carbonatite. In: Bell K., (Ed.) Carbonatites- genesis and evolution. Unwin Hyman, London, 1989, 428–447
[53] Ohde S., Determination of rare earth elements in carbonatites from the Kangankunde Mine, Malawi by instrumental neutron activation analysis. J. Radioanal. Nucl. Ch., 2003, 257(2), 433–435
[54] Wall F., Barreiro B.A., Spire B., Isotopic evidence for late-stage processes in carbonatites: rare earth mineralisation in carbonatites and quartz rocks at Kangankunde, Malawi. Goldschmidt Conference Edinburgh, 1994, 951–952
[55] Wall F., Zaitsev A., Jones A.P., Mariano A.N., Rare-earth rich carbonatites: a review and latest results. J. Geosci., 1997, 42, no. 3, 49
[56] Dowman E., Rankin A.H., Wall F. Fluid and solid inclusion evidence for late-stage mobility of zirconium, titanium and REE in carbonatite systems. ECROFI-XIX, Berne, Switzerland, 2007, Program with abstracts
[57] Rankin A.H., Carbonatite associated rare metal deposits: composition and evolution of ore-forming fluids-the fluid inclusion evidence. In: Linnen R.L., Samson I.M. (Eds.), Rare-Earth Geochemistry and Mineral Deposits, Geological Association of Canada, GAC Short Course Notes, 2005, 17, 299–314
[58] Bühn B., Rankin A.H., Composition of natural, volatile-rich Na–Ca–REE–Sr carbonatitic fluids trapped in fluid inclusions. Geochim. Cosmochim. Acta., 1999, 63, 3781–3797
[59] Ting W., Burke E.A.J., Rankin A.H., Woolley A.R., Characterisation and petrogenetic significance of CO_2, H_2O and CH_4 fluid inclusions in apatite from the Sukulu carbonatite, Uganda. Eur. J. Mineral., 1994, 6, 787–803
[60] Pirogov B.I., Dependence of Technological Properties of the Kovdor Apatite and Heavy Fraction on the Kovdor Ores Peculiarities. Sci. Report, 1987, Krivorozhsky Gornorudny Inst. (in Russian)
[61] Bowers T.S., Helgeson H.C., Calculation of the thermodynamic and geochemical consequences of non ideal mixing in the system H_2O–CO_2–NaCl on phase relations in geologic systems: equation of state for H_2O-CO_2-NaCl fluids at high pressures and temperatures. Geochim. Cosmochim. Acta., 1983, 47, 1247–1275
[62] Bulakh A.G., and Ivanikov V.V., The Problems of Mineralogy and Petrology of Carbonatites. Leningrad University Publ., Leningrad, Russia 1984 (in Russian)
[63] Dennis K.J., and Schrag D.P., Clumped isotope thermometry of carbonatites as an indicator of diagenetic alteration. Geochim. Cosmochim. Acta., 2010, 74, 4110–4122
[64] Ghosh P., Adkins J., Affek H., Balta B., Guo W.F., Schauble E.A., Schrag D., Eller J.M., C-13–O-18 bonds in carbonate minerals: a new kind of paleothermometer. Geochim. Cosmochim. Acta., 2006, 70(6), 1439–1456